Burner Geometry Effects on Combustion and NO_x Emission Characteristics Using a Variable Geometry Swirl Combustor

A. K. Gupta,* M. S. Ramavajjala,† and J. Chomiak‡
University of Maryland, College Park, Maryland 20742
and
N. Marchionna§
Textron Lycoming, Stratford, Connecticut 06497

Results presented here show a significant effect of burner geometry, swirl strength, fuel injector geometry, and input operational parameters on mixing, combustion processes, and emission of trace pollutants. The Variable Geometry swirl Combustor (VGC) described here consisted of six concentric annuli arranged telescopically. The results have been obtained using a configuration in which the fuel is introduced in the central annulus and the air staged through the outer annuli. This paper compares this type of burner with a newer type in which a near premixed fuel and air mixture is introduced close to the burner central axis. The main advantage of this new design is that the centrifugal forces developed by the swirl move the lighter high-temperature burnt gases towards the center of the combustor and the heavier, secondary, and dilution air, which is introduced near the center, towards the outer wall. This results in much better mixing, good pattern factor, high combustion efficiency, low-emission levels, and low pressure drop across the burner. Special emphasis is placed on flow and combustor geometry, which produced very low NO_x emission levels. Results show that very low NO_x levels, coupled with high combustion efficiency, at all burner loadings, can be obtained with this variable geometry combustor. The combustor has the potential for use in gas turbine engines.

Introduction

NITROGEN oxides (NO_x), primarily emitted from the combustion of fossil fuels, play a major role in the formation of photochemical smog and acid rain,[1-3] which are deleterious to the ecological system. It is important therefore, to develop low-emission combustors for application to utility, industrial, and aero gas turbine engine systems, and other propulsion systems. Emphasis is placed on NO_x, which have proved to be the most difficult to remove, of all gaseous pollutants, from combustion. This is partly explained by the fact that they were the last to be recognized as a nuisance, and the obvious steps customarily taken to reduce emissions of CO, unburnt hydrocarbons, and soot tended to maximize NO_x. Although a global understanding of NO_x formation in combustors can be described by the extended Zeldovich mechanism,[1] the NO_x emission can be varied over a large range, at the same burner loading and equivalence ratio, by varying the input operational parameters, position, and geometry of the fuel injector and the geometry of the combustor.[3-9] A particularly flexible system, which allows a comprehensive study of the combustion and emissions of gas turbine type combustors, is the Variable Geometry swirl Combustor (VGC).[8-10] This combustor is in the form of multiconcentric annuli arranged telescopically. The VGC has six concentric annuli arranged to provide co- or counterswirl in any annulus. In this paper, the burner is used with five annuli, and fuel in the form of commercially available natural gas has been used. Capability exists to use liquid fuel in the burner with minimal modifications. Unvitiated air is supplied to each of the annuli via separately controlled flowmeters, this provides control and distribution of the flow and swirl strength precisely.

The results are discussed in two parts. The first part of the paper deals with the investigation of the variable geometry swirl combustor where the fuel is introduced in the central annulus and the air distributed through the surrounding outer annuli. A systematic examination of the effects of the burner geometrical and fluid dynamic parameters has provided large variations in NO_x emission levels at overall similar burner operation conditions. The second part of the paper describes a new type of VGC geometry where the fuel is introduced through one of the outer annuli and the secondary and dilution air through the center. The main advantage of this new design is that the centrifugual forces developed by the swirl move the lighter burnt gases towards the center of the combustor and the heavier, secondary, and dilution air, introduced near the center, towards the outer wall. This arrangement results in enchanced mixing, and yields very uniform temperature and species concentration profiles. A comparative study of the two geometries is made in terms of the flame stability, NO_x emission levels, temperature profiles, and combustion efficiencies, so as to determine the advantages and disadvantages of the new premixed geometry over the previous diffusion flame geometry.

Background on NO_x

The most common oxides of nitrogen that are considered to be pollutants include nitric oxide (NO) and nitrogen dioxide (NO_2). A third oxide, nitrous oxide (N_2O), is extremely stable (about 160 years, as compared to 10 min for NO) and is not considered to be a major pollutant.

Nitrogen oxides (NO_x) are formed in all flame using combustion devices, either by the high-temperature oxidation of atmosphere nitrogen (thermal NO_x), fixation and subsequent oxidation of atmospheric nitrogen via fuel species (prompt NO_x), or by the oxidation of fuel-bound nitrogen compounds (fuel NO_x). For the case of thermal NO_x, the principal re-

Presented as Paper 89-0488 at the AIAA 27th Aerospace Sciences Meeting, Reno, NV, Jan. 9–12, 1989; received March 6, 1989; revision received Sept. 10, 1990; accepted for publication Sept. 12, 1990.

*Professor, The Combustion Laboratory, Department of Mechanical Engineering. Associate Fellow AIAA.
†Graduate Student, The Combustion Laboratory, Department of Mechanical Engineering.
‡Visiting Associate Professor from Institute of Aeronautics, Warsaw, Poland.
§Manager, Combustor Department.

actions are generally recognized to be those proposed by the following three extended Zeldovich mechanisms:

$$N_2 + O \rightleftarrows NO + N \quad (1)$$

$$N + O_2 \rightleftarrows NO + O \quad (2)$$

$$OH + N \rightleftarrows NO + H \quad (3)$$

By assuming steady state for N concentrations, i.e., $d[N]/dt = 0$, the general rate equation for NO by the above three reactions is given by

$$\frac{d[NO]}{dt} = 2K_1[O][N_2]\left[\frac{1 - [NO]^2/K[O_2][N_2]}{1 + K_{-1}[NO]/K_2[O_2] + K_3[OH]}\right]$$

where $K \equiv [(K_1/K_{-1})(K_2/K_{-2})]$ is the equilibrium constant for the reaction $N_2 + O_2 \rightleftarrows 2NO$, and K_i and K_{-i} are the rate constants for the respective reactions in the forward and reverse directions, respectively. For stoichiometric and fuel-lean flames, with proper evaluation of oxygen atom concentration, which often greatly exceeds the equilibrium value, the Zeldovich mechanism [reactions (1) and (2) have been found to adequately predict the emission of thermal nitrogen oxides. Although the mechanism of thermal NO_x is now well-understood, and numerous papers and surveys are available, it is not a trivial task to calculate the amount of NO_x formed from the VGC, or a conventional swirl burner, or even a turbulent diffusion flame. The prediction of NO formation in a flame is based on a number of simplifications, the most important being the separation of the calculation of NO formation rate from the calculation of temperature and concentration fields due to combustion. The nitric oxide kinetics are coupled to combustion kinetics through the provision of the oxygen atom for reactions (1) and (2). Despite this linkage, it is often possible to decouple the calculation of the NO formation rate from that of the combustion rate, because the oxygen atom consumption during the formation of NO is much less than that consumed during the combustion reactions. Apart from this, the amount of NO formed is so small that the heat of reaction associated with nitric oxide formation may be neglected in the calculations of the temperature and concentration fields. In postflame regions, the rate of NO formation in lean premixed hydrocarbon flames can be given by

$$\frac{d[NO]}{dt} = 2K_1K_5[N_2][O_2]^{1/2} \quad (4)$$

where K_5 is the equilibrium constant for reaction

$$\frac{1}{2}O_2 \rightleftarrows O \quad (5)$$

However, in regions near the flame front, the concentration of free radicals and the rates of NO formation are as much as two orders of magnitude higher than those based on equilibrium concentration of reaction (5). The use of superequilibrium concentrations has led to better agreement with the measured rates of NO formation in regions near the flame front. Superequilibrium concentrations of free radicals can be calculated by assuming that the three fast H/O reactions and the CO burnout reaction are equilibrated, i.e.,

$$H + O_2 \rightleftarrows OH + O \quad (6)$$

$$H_2 + O \rightleftarrows OH + H \quad (7)$$

$$H_2 + OH \rightleftarrows H_2O + H \quad (8)$$

$$CO + OH \rightleftarrows CO_2 + H \quad (9)$$

The concentration of oxygen may then be formulated as

$$[O] = \frac{K_6K_8[H_2][O_2]}{[H_2O]} \quad (10)$$

or

$$[O] = \frac{K_6K_9[H_2O][CO][O_2]}{[CO_2]} \quad (11)$$

Either expression for [O] may be used to obtain the rate of NO formation.[14] Thus, knowing the concentrations of stable species, the rate of NO formation may be calculated by using the equilibrium, or partial equilibrium, model for the reaction zone. These models are generally sufficient for predicting NO formation rates in lean premixed hydrocarbon flames.

Caretto[15] argued the use of equilibrium values for atomic and molecular concentrations, by neglecting reaction (3), the following NO time relationship results:

$$[NO] = [NO]_0 + \left(\frac{\alpha}{\beta}\right)(1 - \exp(-\beta t))$$

where

$$\alpha = K_1[O]_{eq}[N_2]_{eq} + K_2[N]_{eq}[O_2]_{eq}$$

and

$$\beta = (K_{-2} + K_1/2)[O]_{eq} + (K_{-1} + K_2/2)[N]_{eq}$$

Samples[16] used the following finite-difference formulation technique to calculate the rate of NO:

$$\frac{1}{r}\left[\frac{\partial}{\partial x}(\rho ur\phi) + \frac{\partial}{\partial r}(\rho vr\phi) - \frac{\partial}{\partial x}\left(r\Gamma_\phi\frac{\partial\phi}{\partial x}\right) - \frac{\partial}{\partial r}\left(r\Gamma_\phi\frac{\partial\phi}{\partial r}\right)\right] = S_\phi$$

where ϕ is the variable NO and $\Gamma_\phi = \mu_{eff}/\sigma_F$.

Thompson et al.[17] provided a satisfying agreement between their experimental results on turbulent diffusion flame and predictions using the following modified rate equation:

$$\frac{d[NO]}{dt} = 1.503 \times 10^{17}\, T^{-1/2}[O_2]^{1/2}[N_2]\, r \exp\left(-\frac{134.7}{RT}\right) \text{ppm/s} \quad (12)$$

where $[O_2]$ and $[N_2]$ are expressed as percentages, and $r = [O]/[O]_{eq}$, derived as $[H_2]/[H_2]_{eq}$.

Equation (12) was used in the present studies to calculate the local NO formation rates in the combustor. The time between two adjacent cells was calculated according to

$$\Delta t_n = \frac{x_n - x_{n-1}}{\bar{u}_m}$$

where $\bar{u}_m$ is the mean velocity given by

$$\bar{u} = \frac{\sum_{j=1}^{m} u_jA_j}{\sum_{j=1}^{m} A_j}$$

By calculating the local values of $[O_2]$, $[N_2]$ and temperature at each node in the combustor (using the FLUENT program),

the local value of [NO] at the node can be evaluated. Therefore, the algorithm for [NO] formation is

$$[NO]_n = [NO]_{n-1} + \left[\left(\frac{d[NO]}{dt}\right) - \left(\frac{d[NO]}{dt}\right)_{n-1}\right]\frac{x_n - x_{n-1}}{\bar{u}_m}$$

with the initial condition of [NO] = 0.

Reduction of NO in the Central Toroidal Recirculation Zone of Flames

Although the generation of thermal NO_x is primarily a temperature-dependent process, it can be controlled (i.e., reduced) by modifications to the flame, using, for example, the fuel-rich or fuel-lean concept, controlled combustion or the availability of rich radical pool species (for destructing NO formed) at desired regions of the flame. In the flame with center core fuel-rich zone, rich chemically active species are produced. Alternatively, a center core fuel-lean flame may be used, since this provides relatively low peak flame temperatures. The role of fuel straining and fuel-air mixing is, therefore, very important from the point of view of NO_x, in addition to combustion efficiency and intensity. The center core lean geometry is particularly attractive for gas turbine applications. The NO_x formation in fuel-rich (or fuel-lean) regions of combustors is negligible, according to the Zeldovich mechanism. In turbulent flames, the degree of swirl imparted to the flow has strong influence on the NO_x emission levels. Evidence of destruction of NO in the central recirculation zone of swirling flames has been found by Sadakata and Beér.[18] Very large residence times[18] and the availability of rich radical pool species, such as those associated with recirculating flows, are believed to be favorable for the destruction of NO. Meyerson[19] proposed the following reaction scheme for the gas phase reduction of nitric oxide in the presence of hydrocarbons and oxygen. Hydrocarbon-free radicals are produced via hydrogen abstraction of the OH radical. This reaction is very rapid, and provides sufficient radicals for NO reduction. It is believed that the reactions involve free radicals, such as substituted and unsubstituted methylidine, CH, methylene, CH_2. For example:

$$CH + NO \rightarrow HCO + N \quad (13)$$

and the competing reaction for the formation of HCN:

$$CH + NO \rightarrow HCN + O \quad (14)$$

The exothermicity of reaction (13) is sufficient to dissociate HCO to CO and H, so that reaction (13) may be written as

$$CH + NO \rightarrow H + CO + N \quad (15)$$

The nitrogen atom formed by reaction (15) can react rapidly with another molecule of NO to yield molecular N_2, according to

$$N + NO \rightarrow N_2 + O \quad (16)$$

Inclusion of the interaction of HCO from reaction (13) with O-atoms and OH radicals along with N-atom recombination, leads to the following global reaction for the reduction of NO:

$$6NO + 4CH \rightarrow 4CO + 2H_2O + 3N_2 \quad (17)$$

Similar reactions have been postulated for the reduction of NO with other intermediate species, such as NH_i, to form N_2.

Emission of NO from Turbulent Diffusion Flames

Although the above schemes represent the kinetic steps in the formation and destruction of NO, pollutant emission levels in practical combustors depend on the simultaneous interaction between the various physical and chemical processes that occur in the combustor. Nitric oxide formation for some simple (predominantly 1-D) cases in lean mixtures is well-understood and predictable. Practical combustors have complex flowfields, and the coupling between fluid dynamics and chemical processes is a major factor in governing combustor performance and the emission of pollutants. At present, our understanding on the details of this interaction is insufficient to permit extrapolation of results obtained from one combustion device to another or to allow quantitative predictions to be made on the effects of the changes in operational parameters on performance of the combustor. It is difficult to assess the limitations of simplified models for practical combustors because of inadequate local flowfield measurements, including turbulence structures and detailed species concentrations serving as test cases that can be used to assess the validity of models. Nevertheless, it is apparent that the flowfield structure, fuel straining in the combustor, and the availability of "radical pool species" are important for achieving ultra low NO_x emission from flames.

In general, NO_x emissions have been handled by preventing their formation, or by converting them in the postflame gases, to N_2 and O_2 by catalytic processes. The most commonly used approach, due to simplicity, is the prevention of NO_x formation by controlled excess air combustion, two- or multistage combustion, exhaust gas recirculation, water injection, modifying geometrical parameters of the burner, controlled combustor operation, etc. This paper concentrates on the effects of geometrical and input parameters on the thermal NO_x emission and optimization of the system for achieving low overall NO_x emission levels. Special emphasis here is on the application of this combustor concept to gas turbine engines.

Experimental Apparatus

The Variable Geometry swirl Combustor (VGC) in the form of telescopic multiconcentric annuli burner makes use of the principle that under turbulent conditions volumetric heat release rates can be controlled by matching the concentrations of reactants in such a way that regions of high fuel concentrations overlap with regions of large shear stresses in the flow. In the following, a brief description is given of the VGC and also of the diagnostics used for the measurement of different parameters, such as NO/NO_x, CO, CO_2, unburnt hydrocarbons, and mean temperatures in flames.

Figure 1 shows a schematic diagram of the VGC used in the parametric studies. The VGC consists of five concentric annuli arranged telescopically. In the results presented here, fuel could be introduced through annulus 1 (innermost) and/or annulus 3. The facility permits fuel and air to be introduced via any combination. The fuel in the form of commercially available natural gas (other gases or liquid fuels can also be used, with minimal modification to the present apparatus) is introduced through the central annulus No. 1, and is injected into the combustor by using injectors of different geometries. Gaseous fuel injection angles can be incrementally varied from 0 (i.e., in the direction of the flow) to 45, 60, or 90 deg to the main flow direction by attaching nozzles containing jets at the desired angle to the exit of the innermost annulus 1. Flow rate through each annulus is monitored using gas flowmeters. The degree of swirl in each annulus (except for the central one) can be independently varied (from 0° to ±75°), thus enabling co- or counterswirl arrangement by simultaneously rotating the swirl vanes in each annulus. The flexibility of changing the swirl in any annulus separately provided the capability for changing the radial distribution of swirl in the combustor.

In order to obtain a representation measure of the emission levels from a given geometry, an extension tube of the same internal diameter as the outermost annulus is attached to the burner exit. The extention tube eliminates the ambient air entrainment into the flame. Combustion gases were sampled at 2.5 and 3.5 burner exit diameters via a water cooled stain-

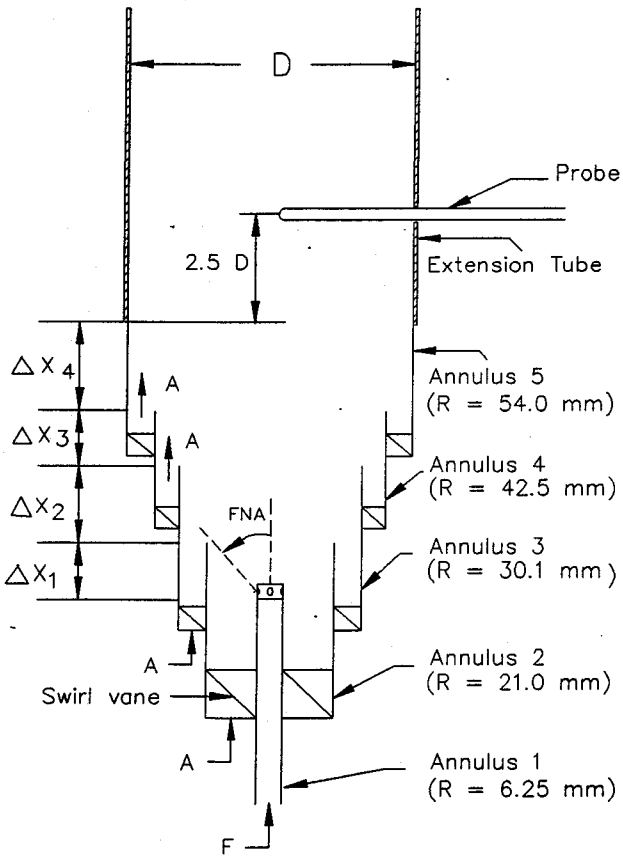

Fig. 1 Schematic diagram of the 5 annuli VGC having diffusion flame configuration.

less steel sampling probe and analyzed for NO/NO_x, using an online Thermo Electron chemiluminescent NO/NO_x analyzer. The sampling train also allowed the simultaneous measurement of CO, CO_2, and unburnt hydrocarbons, using Beckman industrial infrared CO/CO_2 and hydrocarbon analyzers. Water vapor, which interferes with the measurement of the infrared analyzers, is eliminated by using a Perma Pure dryer (placed immediately downstream of the sampling probe) that makes use of a hygroscopic ion exchange membrane. Temperatures are measured using a 0.25 mm bare wire Platinum-Platinum +13% Rhodium thermocouple supported in a ceramic probe.

Numerical Method

Flowfield, combustion, and emission characteristics of the controlled mixing VGC have been evaluated numerically, using the FLUENT code. The code is based on solving the partial differential equations for the conservation of mass, momentum, energy, and chemical species in the gaseous phase by the finite-difference scheme. The detailed governing equations and the solution procedure are given in Refs. 20 and 21. A power law differencing scheme is used for interpolation between grid points, and to calculate the derivatives of the flow variables. Zero-gradient boundary conditions are applied at the axis of symmetry, with the exception of perpendicular velocity components, which must vanish at the axis.

The set of simultaneous algebraic equations are solved at each point by a semi-implicit iterative scheme,[20–23] which starts from arbitrary initial conditions (except at boundaries) and converges to the correct solution (i.e., which satisfies the specified convergence criteria) after performing a number of iterations. The solution is considered to be converged if the cumulative sum of the normalized residues throughout the field for all variables is less than a defined value. The values for this criteria for nonreacting and reacting conditions are chosen to be 10^{-3} and 10^{-4}, respectively. The computational model used is a two-dimensional version of the 3-D FLUENT code, the details of which are given in Refs. 20 and 21. The justification for a 2-D version stems from the axisymmetric nature of the combustor about its longitudinal axis. Local values of O_2, N_2, velocity, and temperature obtained from the numerical code are then used to calculate the local values of NO within the combustor, using Eq. (12).

The finite grid system employed for the combustor had 19 × 35 cells. Calculations have also been carried out using 39 × 69 cells for selected geometries in order to examine the effect of grid size on flowfield, combustion, and NO_x emission characteristics. The expanding grid in the x-direction enables closely packed grid points in regions where large variation in flowfield is expected. The calculations with this arrangement extended to about 2.5 burner exit diameters.

Results and Discussion

Diffusion Flame Geometry

The following geometrical and input parameters were identified to be important input and operational parameters for the VGC:

1) Fuel nozzle injection angle (FNA)
2) Swirl strength in each of the annuli (i.e., radial distribution of swirl in the combustor)
3) Distance between the exit planes of the various annuli, as shown by ΔX_i in Fig. 1
4) Air flow distribution in each of the annuli
5) Fuel flow rate and the corresponding equivalence ratio (ϕ)

In order to obtain favorable combustor geometry for low overall NO_x emission, the extent to which the above parameters influence the NO_x emission levels needs to be examined. This was performed by varying one of the parameters and keeping all the others constant, so that the effect of this parameter on the overall NO_x emission and combustion characteristics could be determined. Repeating this procedure for all the other parameters, low value of overall NO_x emission levels could be achieved. The final results obtained may not be the optimum, due to the possible interaction of one parameter with another. The interaction of fluid dynamics, chemical kinetics, and combustion may lead to some complex chemistry. The global measure of NO_x emission levels also does not provide any information on the local formation and destruction rates. However, significant differences in the flame structure for the flames examined suggests that thermal stratification and fuel/air mixing in the shear layer is very important. Figures 2–5 show some of the results obtained, which

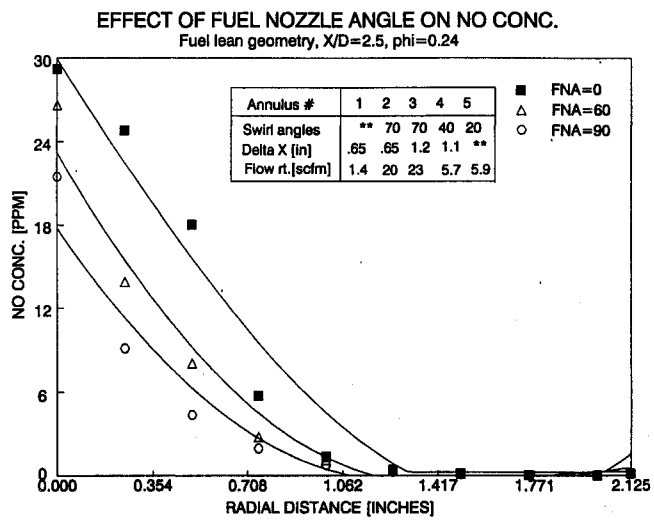

Fig. 2 Effect of fuel nozzle injector geometry on radial distribution of NO concentration at X/D = 2.5, overall equivalence ratio, = 0.24.

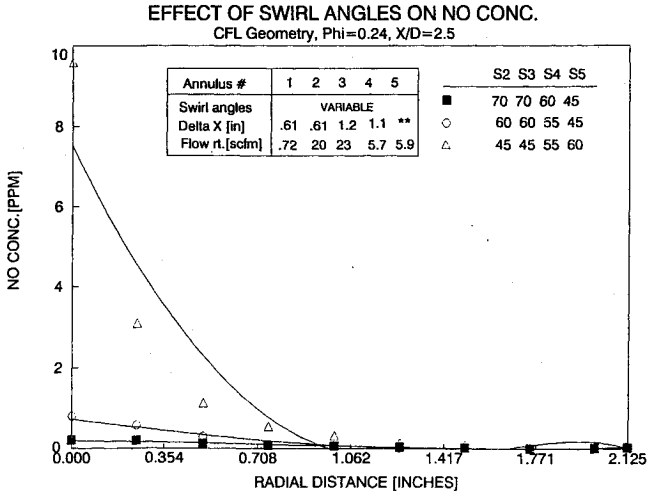

Fig. 3 Effect of radial distribution of swirl in the combustor on NO concentration at X/D 2.5, = 0.24.

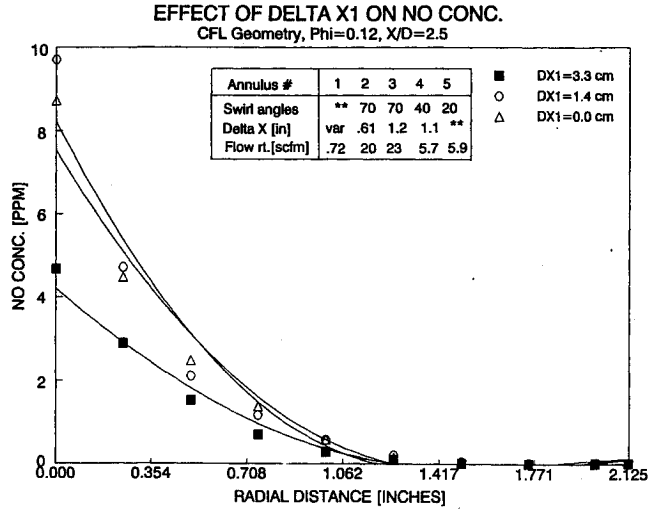

Fig. 4 Effect of X_1 in combustor geometry on NO concentration at X/D = 2.5, = 0.12.

clearly suggest that the flame chemistry and NO_x emission levels are influenced by the combustor geometry and fuel injector design.

The extent of fuel nozzle injector design effects on emission characteristics was determined by attaching fuel nozzles of different designs to the end of the innermost central annulus No. 1. This arrangement facilitated the use of axial, divergent, and radial injection angles of 0, 45, 60, 90 deg to the axis of the burner in the direction of the flow. Figure 2 shows that a fuel nozzle angle of 60 deg yields the lowest value of NO emission for the experimental conditions studied. Strong swirl in annulus 2 and weak swirl in the outermost annulus were found to yield low NO_x emission levels (Fig. 3). These findings provide the important role of initial fuel/air mixing region on NO_x emission. Subsequent experiments were, therefore, conducted with a swirl angle of 60 deg in annulus number 2.

Experimental studies have shown that the swirl has strong effect on the flow field (under both isothermal and combustion conditions), as well as the size, shape, stability, and combustion intensity of the flames.[1,22,24] In the case of strong swirl, the adverse axial pressure gradient is sufficiently large to result in static pressure deficit along the axis, resulting in flow recirculation and the formation of an internal recirculation zone. Evidence of the destruction of NO in the internal recirculating zone of swirling flames has been found by Sadakata and Beér.[18] Figure 3 supports this statement.

Figure 4 shows the effect of ΔX_1 on NO concentration. As Δx_1 is increased, NO concentration decreases. However, in combustors where compactness is important, very large ΔX is not an acceptable solution. For small values of ΔX_2, NO concentration remains practically unaffected. But, as ΔX_2 is increased (beyond 5 cm for the present experimental conditions), the flame experiences more confinement, which is expected to yield higher temperatures and, consequently, higher levels of thermal NO.

Having examined the effect of individual parameters on overall NO_x emission levels, the next step was to determine the precise species concentration and the corresponding combustion efficiencies. The results presented in Figs. 6 and 7 reveal that, as equivalence ratio increases, temperature increases, with the result that thermal NO increases. The trends for calculated and experimental results are similar. The discrepancy between measured and calculated NO could be due to the lack of agreement for mean temperatures. A better prediction of temperature would lead to better agreement for thermal NO. Our present efforts are aimed in this direction for a range of conditions. Figure 8 shows the combustion efficiency, corresponding to conditions shown in Figs. 6 and 7, evaluated from CO and CO_2 measurements. For Hydrocarbon fuels, the ratio between net CO_2 and gross CO_2 gives a very good estimate of the combustion efficiency, indicating that the burner has a maximum efficiency at an approximate input equivalence ratio of ϕ = 0.2.

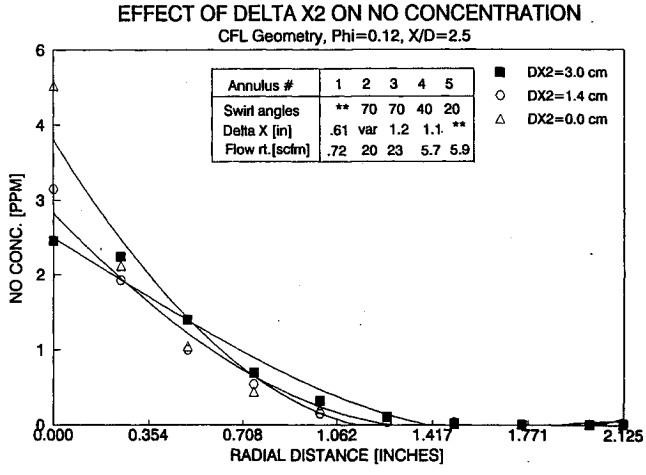

Fig. 5 Effect of X_2 in combustor geometry on NO concentration at X/D = 2.5, = 0.12.

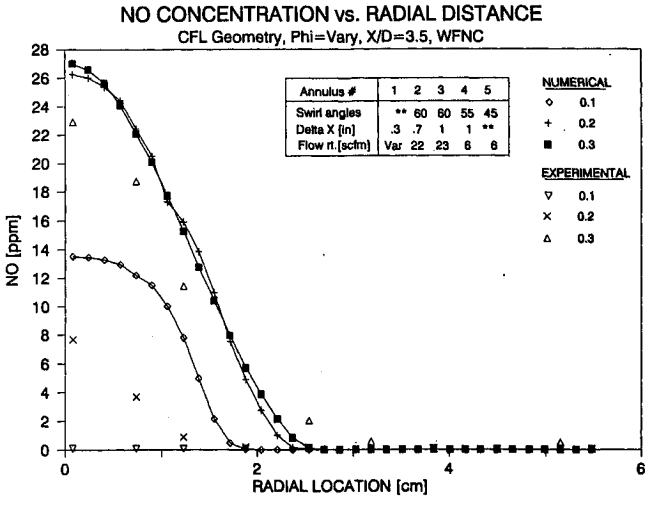

Fig. 6 Radial distribution of NO at = 0.1, 0.2, and 0.3 and its comparison with calculations at X/D = 2.5.

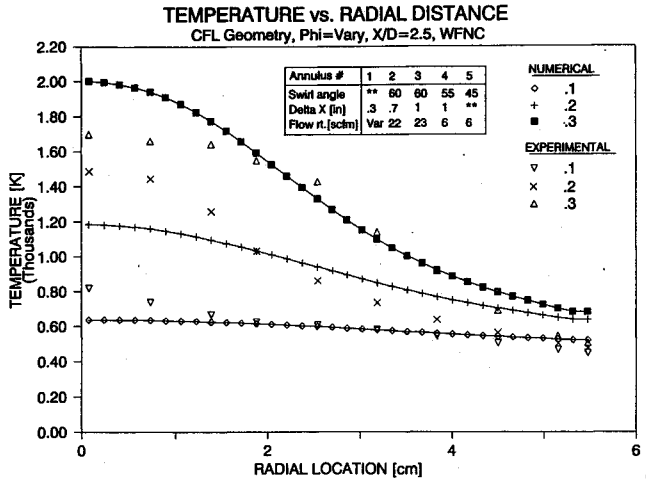

Fig. 7 Radial distribution of temperature at = 0.1, 0.2, and 0.3 and its comparison with calculations at X/D = 2.5.

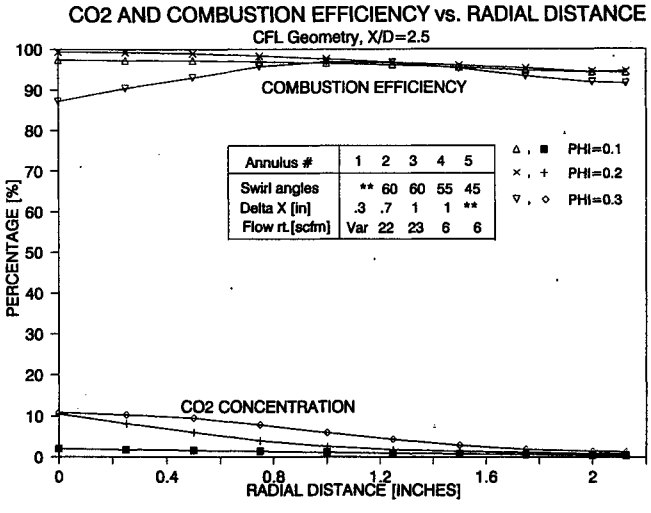

Fig. 8 Radial distribution of CO_2 and combustion efficiency at = 0.1, 0.2, and 0.3 at X/D = 2.5.

Premixed Geometry

It is important to perceive that the flames obtained from the previous burner geometry are of the diffusion type. In these flames, even though the overall fuel/air ratio may be lean, the temperatures of these flames are near stoichiometric value, at least during part of the burning zone near the fuel-air interface. Hence, more NO_x is expected to be formed in the diffusion flames than that calculated based on the equilibrium temperature from the overall equivalence ratio. Moreover, the reduction reactions of NO are so slow that, in most practical systems, the amount of NO formed in diffusion flames is unaffected by the subsequent decrease in temperature caused by dilution of the products with excess air. With this motivation, a new burner geometry was conceived (Fig. 9) in which near premixed flames are obtained. In this configuration, premixed fuel-air mixture is introduced through annulus 3, and the unvitiated air through annuli 2, 4, and 5. This arrangement results in a radial density stratification, because the density first decreases and then increases, with the progressive increase in radial distance from the central axis of the burner to the burner outer walls. The combined effect of rotation and density stratification results in buoyancy-induced instability of the flow, with the net result of enhanced mixing. The flame stability was examined in order to establish the stable range of burner operation with this new design. This was carried out by fixing a certain constant velocity in all the annuli, and then decreasing the fuel equivalence ratio until the flame blow-off occurred. Figure 10 shows that the premixed geometry is more stable than the diffusion flame geometry, except at low Reynolds number. The inherent nature of the diffusion process keeps the flame stable at low Reynolds number. A comprehensive graph of the stability for much higher Reynolds number could not be obtained, due to compressed air and fuel supply limitations. The effect of swirl in annulus 3 on the stability was studied, and the results shown in Fig. 11 reveal that the burner is most stable at near 50 deg swirl angle.

A preliminary examination of the new premixed geometry configuration gave very encouraging results in terms of NO_x emission, radial temperature profiles, and combustion efficiencies. The enhanced mixing rate caused by rotation and density gradient results in near uniform radial distributions of temperature and species concentration. Figure 12 provides

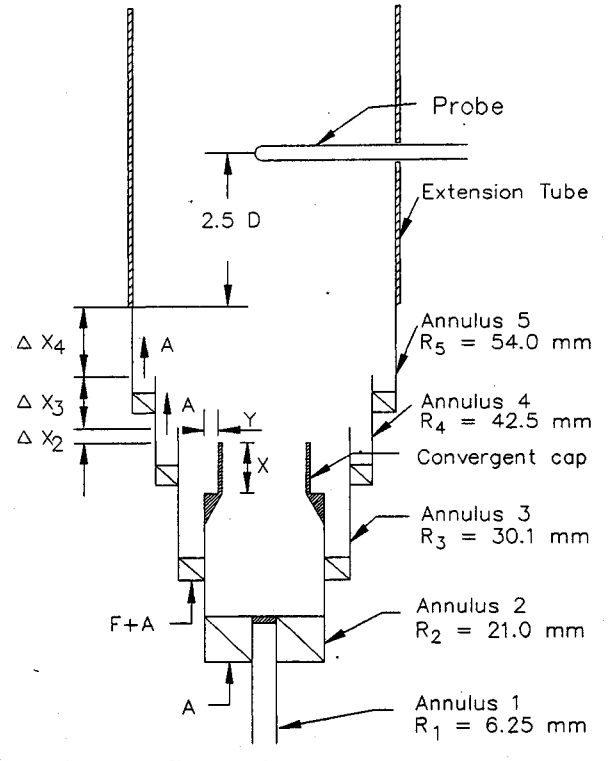

Fig. 9 Schematic diagram of the premixed geometry combustor in the form of variable geometry swirl combustor.

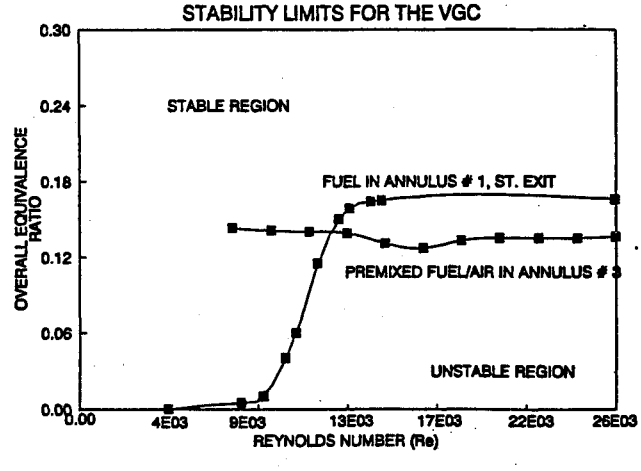

Fig. 10 Comparison of stability limits for diffusion flame and premixed flame configuration of variable geometry swirl combustor.

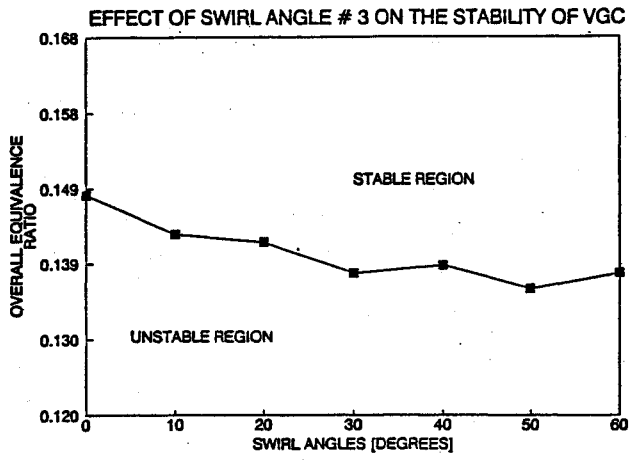

Fig. 11 Comparison of stability limits for diffusion flame and near premixed flame configuration of variable geometry combustors.

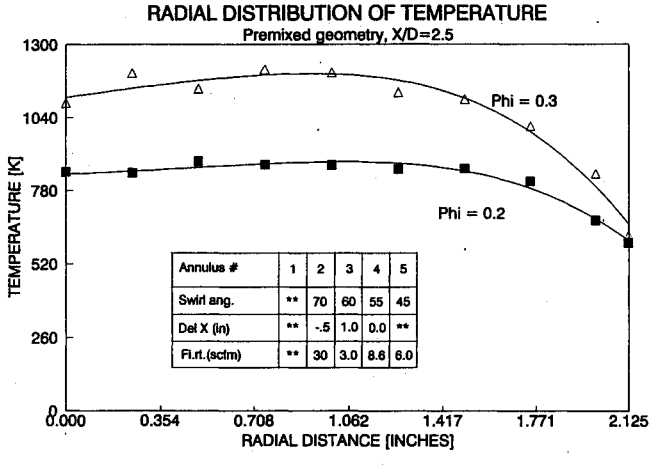

Fig. 12 Radial distribution of temperature for = 0.2 and 0.3 at X/D = 2.5 in the premixed VGC.

the radial temperature distribution at equivalence ratios of ϕ = 0.2 and ϕ = 0.3. The curves are fairly uniform throughout, except near the wall where the temperatures are lower because of rapid dilution of the hot gases with the cooling air that is introduced in the outermost annulus and the burner outer wall quenching effects. The temperature distribution for the diffusion flame geometry for the same equivalence ratio is very nonuniform (approximates a near Gaussian distribution), with maximum value close to the central axis of the burner. The NO_x profiles are indeed uniform, as shown in Fig. 13, and the combustion efficiencies are very high (Fig. 14). Tables 1 and 2 give a comparison of the two geometries. The results reveal that the above premixed geometry can provide lower NO_x values coupled with high combustion efficiency, good stability limits, and uniform burner exit temperature profiles. Further studies in this direction to generalize these findings will enrich our knowledge for developing design strategies for low NO_x combustors.

Conclusions

The results from the parametric studies have shown the importance of the burner and fuel nozzle injector geometry parameters in the Variable Geometry swirl Combustor on the emission and combustion characteristics. A new burner geometry is identified that has provided good stability limits, high combustion efficiency, uniformity in concentration profiles, and good pattern factor (uniform radial distribution of mean temperatures) downstream of the burner exit. Future studies in this area include systematic examination of the new

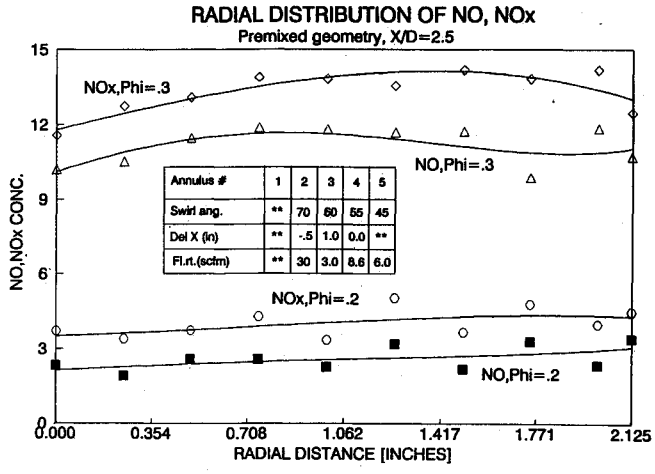

Fig. 13 Radial distribution of NO and NO_x for = 0.2 and 0.3 at X/D = 2.5 in premixed VGC.

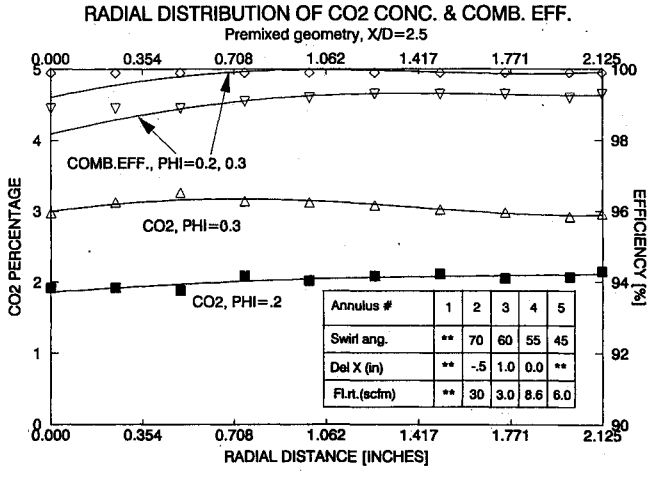

Fig. 14 Radial distribution of CO_2 and combustion efficiency for = 0.2 and 0.3 at X/D = 2.5 in premixed VGC.

Table 1 Geometric and combustion data for the central core fuel lean diffusion flame VGC

Geometry					
Annulus number	1	2	3	4	5
Swirl angle, deg	0	60	60	55	45
Delta X, in.	0.3	0.7	1.0	1.0	N/A
Flow rate, schm	Variable	22	23	6.0	6.0
Combustion Data for the VGC at X/D = 2.5					
ϕ	NO, ppm	NO_x, ppm	CO, ppm	CO_2, %	η, %
0.1	0.177	0.52	375	1.03	96.4
0.2	0.888	2.585	592	2.12	97.28
0.3	1.168	3.746	2274	2.926	92.8
0.35	2.69	6.106	4791	3.196	86.9
Combustion Data for the VGC at X/D = 3.25					
ϕ	NO, ppm	NO_x, ppm	CO, ppm	CO_2, %	η, %
0.1	0.199	0.549	256	1.02	97.5
0.2	0.724	2.598	514	2.533	97.9
0.3	1.171	3.681	1333	3.873	96.7
0.35	2.626	6.126	2273	5.025	95.6

Table 2 Geometric and combustion data for the premixed flame in the VGC. The cap located at the exit of annulus 2 had a step height-to-length ratio (x/y) of 8.8

Geometry					
Annulus number	1	2	3	4	5
Swirl angle, deg	0	70	60	55	45
Delta X, in.	0	−0.5	1.0	0.0	N/A
Flow rate, schm	0	30	3.0	8.6	6.0
Combustion Data for the VGC at X/D = 2.5					
ϕ	NO, ppm	NO_x, ppm	CO, ppm	CO_2, %	η, %
0.2	0.011	1.162	163.8	2.08	99.22
0.3	0.164	3.03	28.05	3.14	99.9

premixed geometry (in addition to the diffusion flame geometry) for NO_x emission and combustion characteristics at various conditions, in particular, near to the region of nozzle(s) exit, in addition to the mathematical modeling studies. Future plans also include increasing the number of annuli to six, and examining the burner characteristics with liquid fuels. This comprehensive study of the NO_x emissions and flame behavior will help combustion engineers in the design and development of a new generation of compact gas turbine combustors, aimed for ultra low emissions and high combustion efficiency.

Acknowledgments

The financial support provided by Textron Lycoming and the University of Maryland is gratefully acknowledged. The FLUENT code used here was provided by Creare Inc. and is much appreciated.

References

[1]Gupta, A. K., Lilley, D. G., and Syred, N., *Swirl Flows*, Abacus Press, Tunbridge Wells, Kent, England, 1984.

[2]Elliot, C. T., and Schwieger, R. G., *The Acid Rain Source Book*, McGraw Hill, New York, 1984.

[3]Beér, J. M., and Headley, A. B., "Reduction of Combustion General Pollution," *Proceedings of Fuel and Environment Conf.*, The Institute of Energy, U.K., Vol. 1, Nov. 1973, pp. 67–180.

[4]Heap, M. P., Lowes, T. M., and Walmsley, R., "Emission of NO from Large Turbulent Diffusion Flames," *Proceedings of 14th International Symposium on Combustion*, The Combustion Institute, Pittsburgh, PA, 1973, pp. 883–895.

[5]Gupta, A. K., Ong, L. H., and Marchiona, N., "NO_x Reduction and Combustion Phenomenon in a Multi-Annular Gas Turbine Swirl Burner," AIAA/SAE/ASME/ASEE Joint Propulsion Conf., San Diego, CA, June 29–July 2, 1987, Paper No. 87–2036.

[6]Gupta, A. K., and Razavi, R. M., "Flowfield and Combustion Phenomenon in the Multi-Annular Swirl Burner for NO_x Reduction," AIAA 26th Aerospace Science Meeting, Reno, NV, Jan. 1988, Paper No. 88–1054.

[7]Gupta, A. K., Beér, J. M., and Swithenbank, J., "On the Operational Characteristics of a Multi-Annular Swirl Burner," Central States Section, The Combustion Institute Meeting, Cleveland, OH, March, 1977.

[8]Gupta, A. K., Beér, J. M., and Swithenbank, J., "Concentric Multi-Annular Swirl Burner: Stability Limits and Emission Characteristics," *Proceedings of 16th International Symposium on Combustion*, The Combustion Institute, Pittsburgh, PA, 1977, pp. 79–91.

[9]Gupta, A. K., Razavi, R. M., and Chomiak, J., "Experimental and Theoretical Studies in the Controlled Mixing Variable Geometry Combustor," AIAA/ASME/SAE/ASEE 24th Joint Propulsion Conf., Boston, MA, July 11–13, 1988, Paper No. 88–2857.

[10]Beér, J. M., British Patent No. 1099959, 1968.

[11]Bowman, C. T., *Emissions from Continuous Combustion Systems*, edited by W. Cornelius and W. G. Agnew, Plenum Press, New York, 1970, p. 98.

[12]Fenimore, C. P., "Reactions of Fuel-Nitrogen in Rich Flame Gasses," *Combustion and Flame*, Vol. 26, 1976, pp. 249, see also *Proceedings of 13th International Symposium on Combustion*, The Combustion Institute, Pittsburgh, PA, 1971, p. 373.

[13]Jones, R. E., "Gas Turbine Engine Emissions Problems, Progress and Future," *Progress in Energy and Combustion Science*, Vol. 4, edited by N. Chigier, Pergamon Press, U.K., 1978, pp. 73–113.

[14]Iverach, D., Basden, K. S., and Kirov, N. Y., "Formation of Nitric Oxide in Fuel-Lean and Fuel Rich Flames," *Proceedings of 14th International Symposium on Combustion*, The Combustion Institute, Pittsburgh, PA, 1973, pp. 767–775.

[15]Caretto, L. S., "Modeling Pollutant Formation in Combustion Processes," *Proceedings of 14th International Symposium on Combustion*, The Combustion Institute, Pittsburgh, PA, pp. 803–817.

[16]Samples, J. W., *Prediction of Axisymmetric Chemically Reacting Combustor Flowfields*, Ph.D. Thesis, Oklahoma State Univ., Stillwater, OK, May 1983.

[17]Thompson, D., Brown, T. D., and Beér, J. M., "Formation of NO in a Methane-Air Flame," *Proceedings of 14th International Symposium on Combustion*, The Combustion Institute, Pittsburgh, PA, 1973, pp. 787–799.

[18]Sadakata, M., and Beér, J. M., "Spatial Distribution of Nitric Oxide Formation Rates in Swirling Turbulent Methane Air Flame," *Proceedings of 16th International Symposium on Combustion*, The Combustion Institute, Pittsburgh, PA, pp. 93–103.

[19]Meyerson, A. L., "The Reduction of Nitric Oxide in Simulated Combustion Effluent by Hydrocarbon-Oxygen Mixtures," *Proceedings of 15th International Symposium on Combustion*, The Combustion Institute, Pittsburgh, PA, 1975, pp. 1085–1092.

[20]Modarres-Razai, M. R., and Gupta, A. K., "Effect of Swirl and the MASB Geometry on Flowfield and Combustion Characteristics," *Proceedings of ASME Computers in Engineering Conf. and Exhibition*, New York, Aug. 9–13, 1987, pp. 159–171.

[21]*Creare Inc. FLUENT Code Users Manual for Version 2.96*, Hanover, NH, 1988.

[22]Gupta, A. K., Lilley, D. G., and Syred, N., *Swirl Flows*, Abacus press, Tunbridge Wells, Kent, England, 1984.

[23]Gupta, A. K., and Lilley, D. G., *Flowfield Modeling and Diagnostics*, Abacus Press, Tunbridge Wells, Kent, England, 1985.

[24]Mestre, A., and Benoit, A., *Combustion in Swirling Flow*, Office National D'Etudes et de Recherches Aerospaciles, Chatillon, France.